Application Report

SLUAA38–June 2020

Single-Event Effects (SEE) Test Report of the UC1825B-SP High Speed PWM Controller

ABSTRACT

The purpose of this study is to characterize the single-event-effect (SEE) performance due to heavy-ion irradiation of the UC1825B-SP. Heavy-ions with LET_{EFF} ranging from 20 to 74 MeV·cm^2/mg were used to irradiate production RHA devices in 15 experiments with fluences ranging from 10^6 to 10^7 per run. The results demonstrated that the UC1825B-SP device is SEL-free up to 74 MeV·cm^2/mg at T = 125°C, SEB-free up to 74 MeV·cm^2/mg at room temperature, and across the full electrical specifications. The UC1825B-SP device is also SET-free for V_{OUT} SET ≥ |3.5%| from the nominal output voltage of 5 V. The SET cross section for the PWM (output) is presented and discussed.

Contents

List of Figures

List of Tables

Trademarks

1 Introduction

The UC1825B-SP control IC is a pin-for-pin compatible, TID radiation-improved version of the UC1825-SP device. Providing the necessary characteristics to control current-mode and voltage-mode power supplies. Some of the features of this device are:

- 50-ns propagation delay-to-output
- 1.5-A peak totem pole outputs for capacitive load.
- Practical switching frequencies up to 1MHz.
- Wide-Bandwidth Error Amplifier
- Soft Start/Maximum Duty-Cycle Control
- Pulse-by-Pulse Current Limiting

The controller can support various DC-to-DC topologies such as the following:

- Flyback
- Forward
- BuckBoost
- Push Pull
- Half-Bridge (using external interface I.C.)
- Full-Bridge (using external interface I.C.)

The device is offered in a thermally-enhanced 16-pin ceramic, dual in-line flat package. Table 1 lists the general device information and test conditions. Visit the UC1825B-SP product page for more detailed technical specifications, user's guides, and applications notes.

Table 1. Overview Information [(1)]

DESCRIPTION	DEVICE INFORMATION
TI Part Number	UC1825B-SP
Orderable Name	5962R8768106VYC
Device Function	Current-Mode PWM Controller
Technology	JI
Exposure Facility	Radiation Effects Facility, Cyclotron Institute, Texas A&M University and Lawrence Berkeley 88-Inch Cyclotron, University of California at Berkeley
Irradiation Temperature	25°C and 125°C (For SEL Testing)

(1) TI may provide technical, applications or design advice, quality characterization, and reliability data or service. Providing these items shall not expand or otherwise affect TI's warranties as set forth in the Texas Instruments Incorporated Standard Terms and Conditions of Sale for Semiconductor Products and no obligation or liability shall arise from Semiconductor Products and no obligation or liability shall arise from TI's provision of such items.

2 Single-Event Effects

One test that was done on the UC1825B-SP is testing its resilience against the destructive single event effects (DSEE): single-event latch-up (SEL) and single event burnout (SEB). The UC1825B-SP is a bipolar-only process. The bipolar process allows the controller to be virtually SEL-free. However, the device was still checked for SEL. For testing, the device was powered at the absolute maximum voltage at VCC = 30 V and heated to approximately 125°C. No current fluctuation outside of the normal behavior was observed during the exposure with heavy-ions up to 75 MeV·cm^2/mg, fluence of 10^7 ions/cm^2, and a die temperature of approximately 125°C.

Since BJT devices can suffer SEB [(1), (2)] the UC1825B-SP was tested at the absolute maximum input voltage for burnout. No current increase was observed, demonstrating that the UC1825B-SP is SEB-free across the full electrical specifications and up to 75 MeV·cm^2/mg, fluence of 10^7 ions/cm^2 at room temperature.

In addition to the destructive behavior, the UC1825B-SP was evaluated for Single-Event-Transients (SET). In any electronic circuit, the passage of heavy ion through the active areas of the silicon can result in transient charge collection. This charge collection ultimately affects circuit behavior by moving internal voltage nodes, affecting overall circuit behavior. In any power supply application, the proper operation of down-stream circuits are tied to the robustness and integrity of the rails. Transient events must be bounded and short in duration for the system to tolerate them. The UC1825B-SP was characterized for SET on the output when using the controller in a push-pull topology. The Pulse-Width-Modulated (PWM) output signal was characterized for output duty cycle changes that exceed ±6% from the nominal value as well as separately characterized for changes that exceed ±25% from the nominal value. In addition, the output of the push-pull converter was tested for changes that exceeded ±3.5% although none were found. These signals are characterized, discussed, and summarized in detail in this report. Furthermore, for each of the different single-event effects, an in-orbit rate for LEO and GEO (ISS) using worst-week method is presented for reference.

3 Test Device and Evaluation Board Information

The UC1825B-SP device is packaged in a 16-pin, thermally-enhanced, dual-ceramic, flat pack package (HKU) as shown in Figure 1. The UC1825BEVM-CVAL evaluation board was used to evaluate the performance and characteristics of the UC1825B-SP under heavy-ions. Figure 2 shows the top views of the evaluation board used for the radiation testing. Figure 3 and Figure 4 show the board schematics for the EVM as used for the heavy-ion testing. See the UC1825B-SP Evaluation Module for more information about the evaluation board.

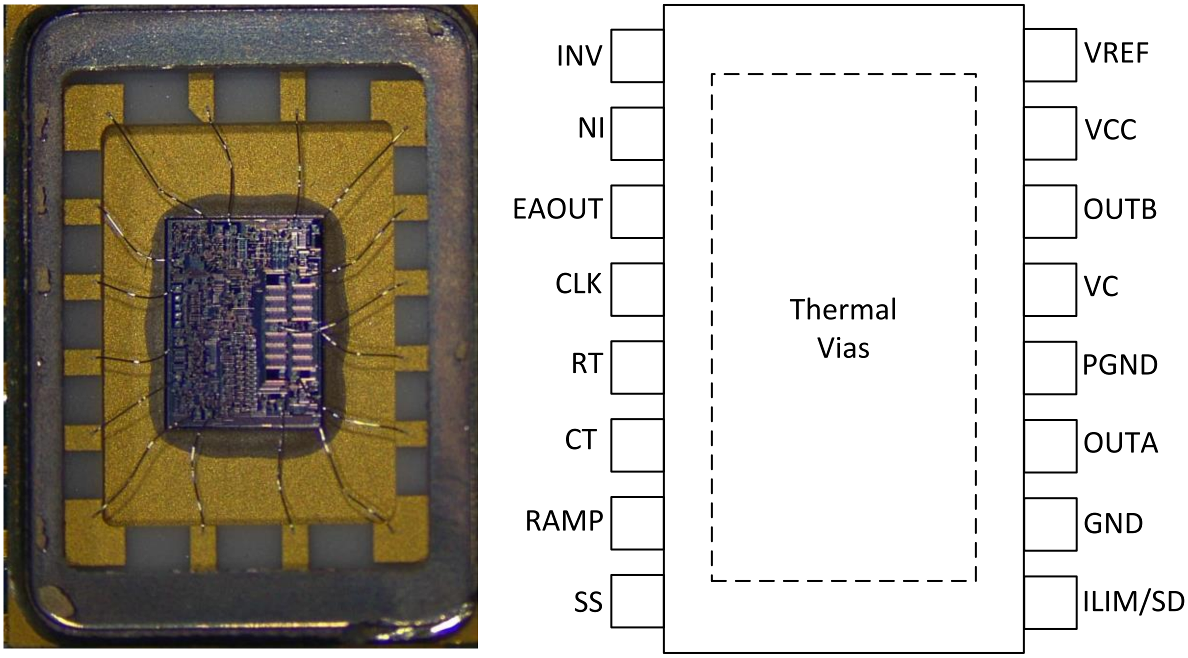

The package lid was removed to reveal the die face for all heavy-ion testing.

Figure 1. Photograph of De-lidded UC1825B-SP [Left] and Pinout Diagram [Right]

Figure 2. UC1825B-SP EVM Top View

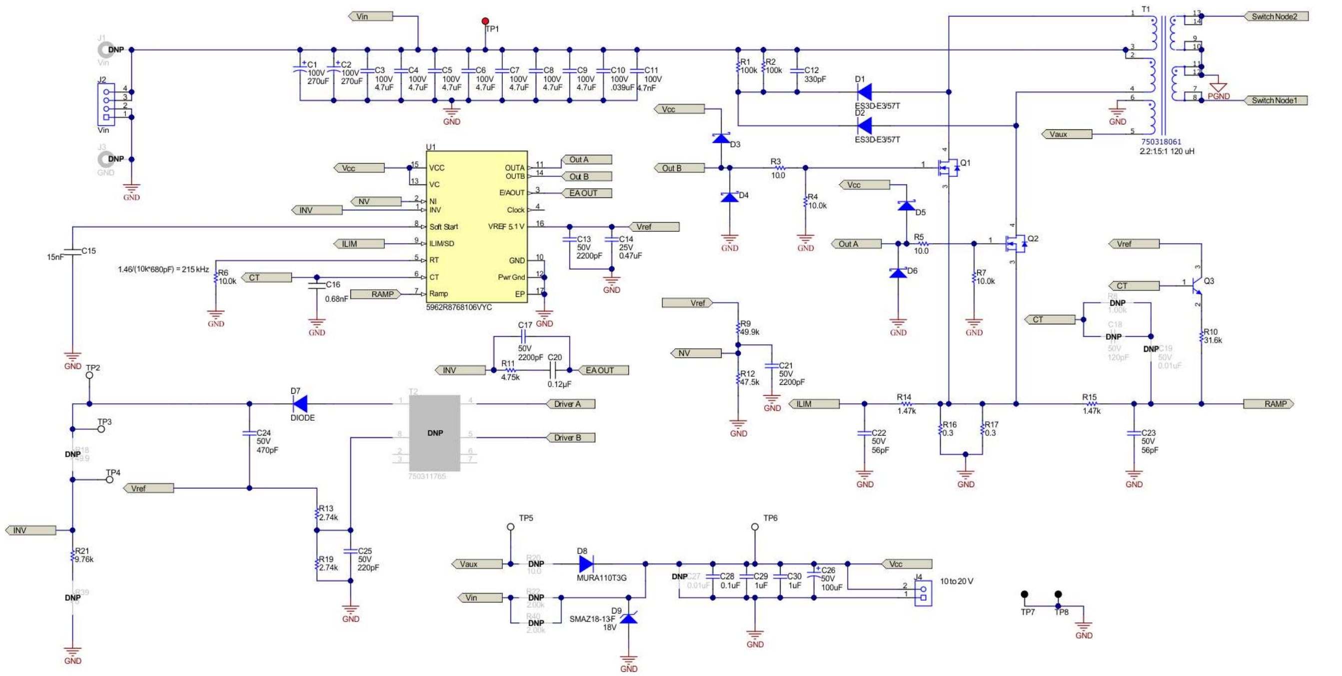

Figure 3. Page 1 of the Schematics of the UC1825BEVM-CVAL EVM as Used for the Heavy-ion Testing Campaign

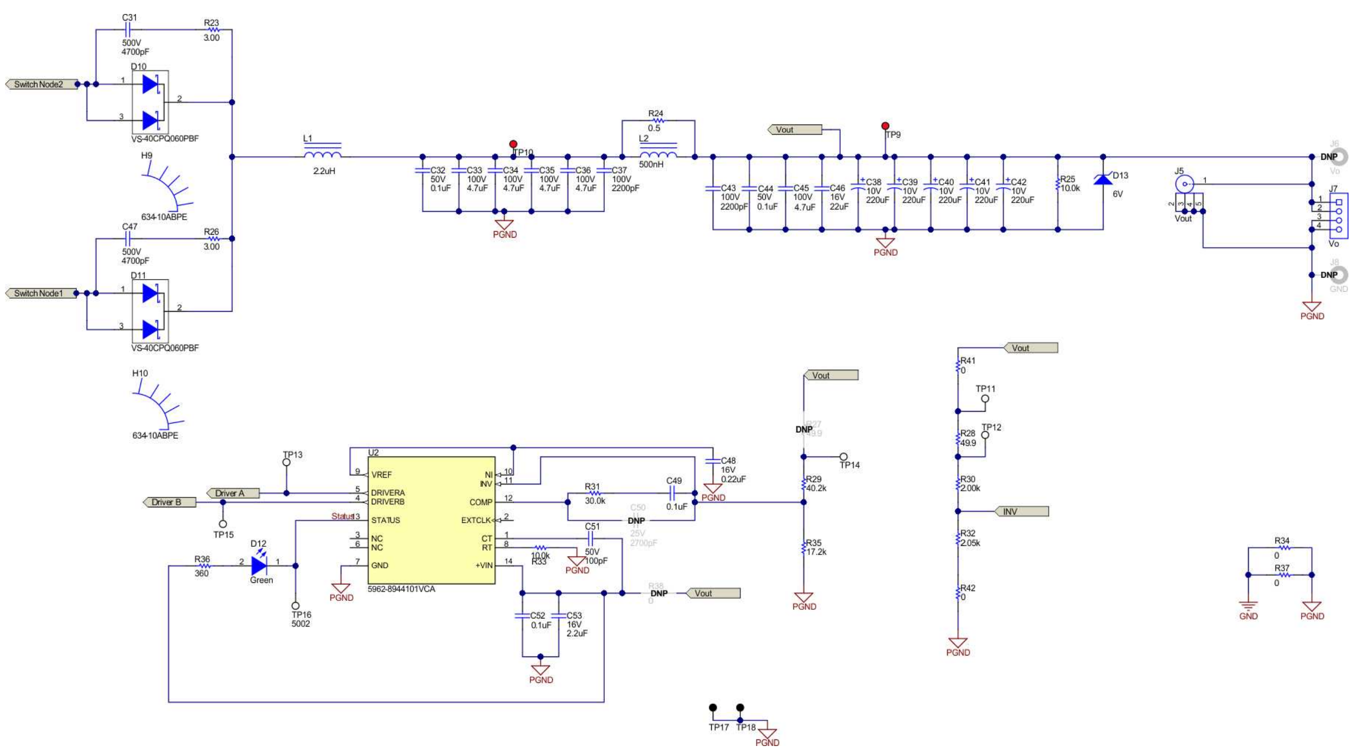

Figure 4. Page 2 of the Schematics of the UC1825BEVM-CVAL EVM as Used for the Heavy-ion Testing Campaign

4 Irradiation Facility and Setup

The heavy-ion species used for the SEE studies on this product were provided and delivered by the TAMU Cyclotron Radiation Effects Facility [(3)] and the 88-Inch Berkeley Accelerator Space Effects (BASE) Facility[(4),(5)], using a superconducting cyclotron and an advanced electron cyclotron resonance (ECR) ion source. At the fluxes used, ion beams had good flux stability and high irradiation uniformity over a one inch diameter circular cross-sectional area for the in-air station (TAMU).

Uniformity is achieved by magnetic defocusing. The flux of the beam is regulated over a broad range spanning several orders of magnitude. For the bulk of these studies, ion flux of 10^4·s and 10^5 ions/cm^2·s were used to provide heavy-ion fluences of 10^6 and 10^7 ions/cm^2.

For the experiments conducted on this report, ^{63}Cu ions at angles of 0º and 50º of incidence were used for an LET_{EFF} of 20 and 31.3 MeV·cm^2/mg, respectively. ^{109}Ag ions at angles of 0º , 30º, and 50º of incidence were used for an LET_{EFF} of 47 and 54.5 and 74 MeV·cm^2/mg, respectively. Also, ^{124}Xe ions at angles of 35º of incidence were used for an LET_{EFF} of 74 MeV·cm^2/mg. The total kinetic energy of ^{63}Cu and ^{109}Ag in the vacuum are 0.944 and 1.63 GeV, respectively at 15 MeV/nucleon (TAMU). For ^{124}Xe the kinetic energy is 1.24 GeV at 10 MeV/nucleon (Berkeley). Ion uniformity for these experiments was between 95% and 98%.

Figure 5 shows the UC1825B-SP test board used for the experiments at the TAMU facility. Although not visible in this photo, the beam port at TAMU has a 1-mil Aramica window to allow in-air testing while maintaining the vacuum within the accelerator with only minor ion energy loss. Test points were soldered on the back for easy access of the signals while having enough room to change the angle of incidence and maintaining the 40 mm distance to the die. The in-air gap between the device and the ion beam port window was maintained at 40 mm at all times.

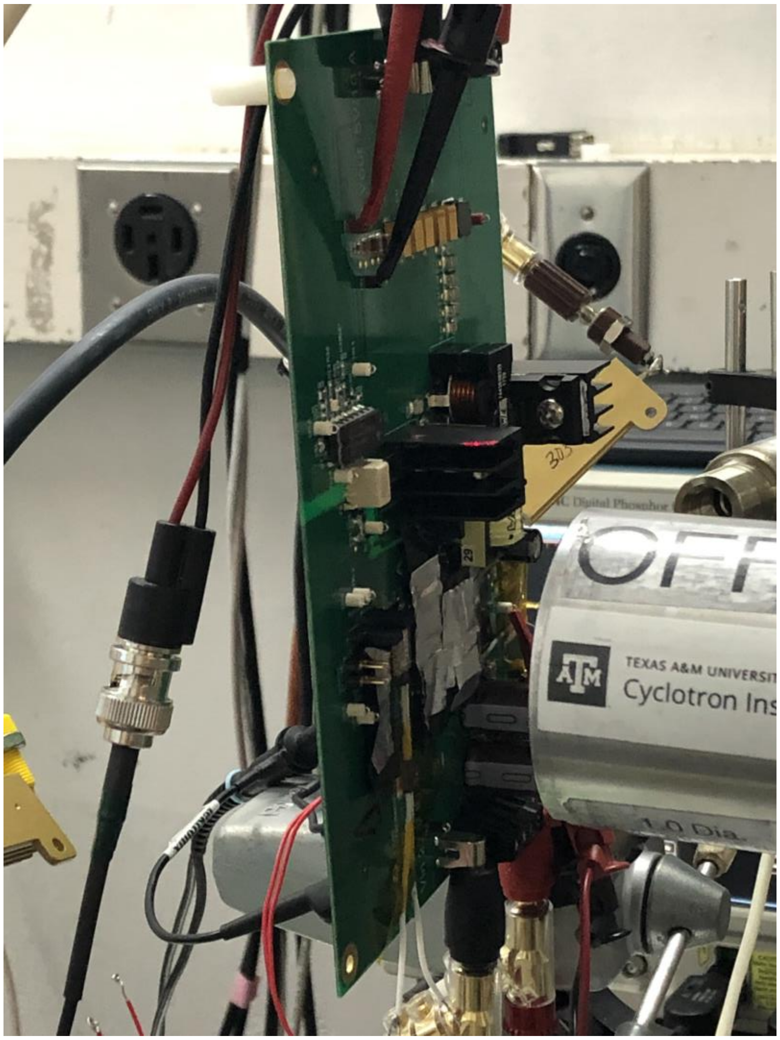

Figure 5. Photograph of the UC1825B-SP Mounted on the UC1825BEVM-CVAL EVM in Front of the Heavy-ion Beam Exit Port at the TAMU Accelerator Facility

5 Depth, Range, and LET$_{EFF}$ Calculation

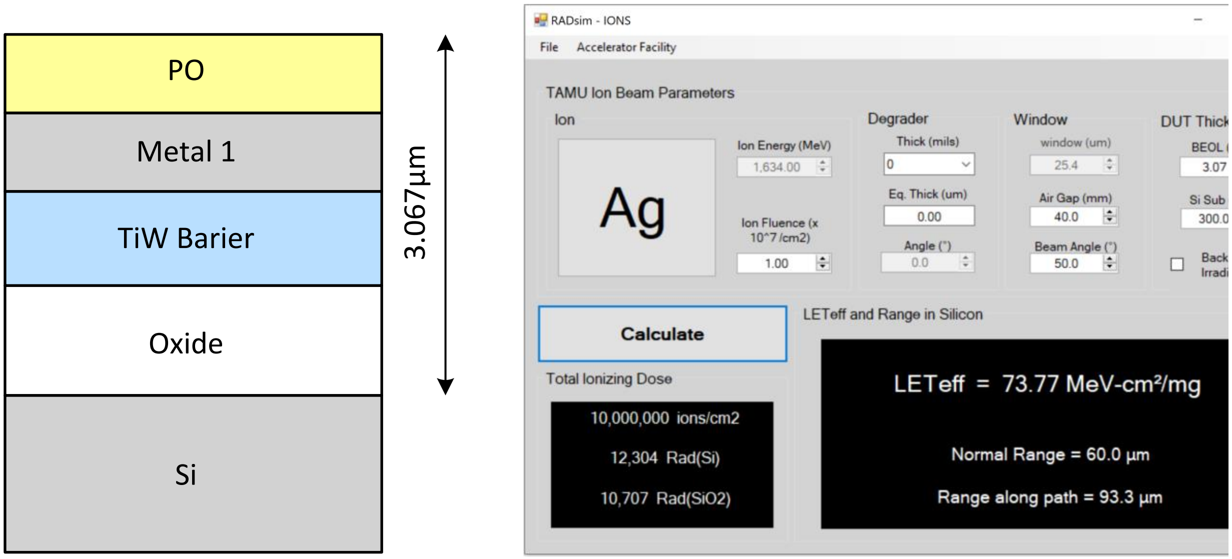

Figure 6. Generalized Cross Section of the JI Technology BEOL Stack on the UC1825B-SP [Left] and GUI of RADsim Application Used to Determine Key Ion Parameter [Right]

The UC1825B-SP device is fabricated in the Texas Instruments Linear JI process with a back-end-of-line (BEOL) stack consisting of one level of standard thickness aluminum metal. Since LET for any given ion is largely a function of the material density through which the ion is traveling, and since the density of aluminum (2.70 g/cm^3) and silicon oxide (2.65 g/cm^3) are similar, the stack is modeled as a homogenous layer of silicon dioxide. The thickness from the surface of the passivation to the silicon surface is 3.067 µm (based on nominal thickness layer) as shown in Figure 6.

The left side of Figure 6 shows a generalized JI technology BEOL stack on the UC1825B-SP cross section. The right side of the image shows the GUI of the RADsim-IONS (based on SRIM) applications used to determine key ion parameters such as LET$_{EFF}$, depth and range for a given ion type, energy, stack, and facility. The application accounts for the 1-mil thick Aramica (DuPont™ KEVLAR®) and the distance from the DUT (in this case 40 mm) to the output nozzle for the Texas A&M Facility. Table 2 shows the results for the ions used for the purpose of UC1825B-SP SEE characterization.

Table 2. LET$_{EFF}$ Depth and Range for the Ions Used for SEE Characterization of the UC1825B-SP

ION TYPE	ANGLE OF INCIDENCE (°)	DEPTH IN SILICON (µm)	RANGE IN SILICON (µm)	LET$_{EFF}$ (MeV·cm^2/mg)	FACILITY
^{63}Cu	0	120.4	120.4	20	TAMU
^{63}Cu	50	76.3	118.7	31.3	TAMU
^{109}Ag	0	95	95	47.1	TAMU
^{109}Ag	30	81.9	94.6	54.48	TAMU
^{109}Ag	50	60	93.3	73.8	TAMU
^{124}Xe	35	69.7	85.1	74.1	Berkeley

6 Test Setup and Procedures

SEE testing was performed on a UC1825B-SP device mounted on a UC1825BEVM-CVAL board. The power stage (V_{IN}) was powered by using the J1 (V_{IN}) and J3 (GND) banana inputs. The UC1825B-SP (V_{CC}) power was provided by using the J4 terminal block. V_{CC} and V_{IN} were provided using channel #3 and #4 of an N6702 precision power supply, respectively. The model of PS channels used are:

- Channel #3 model: N6776A
- Channel #4 model: N6775A

Aluminum tape was used to cover and prevent all active circuitry in the vicinity of the UC1825B-SP from being exposed to the heavy-ions. For all data collected and discussed in this report, the output voltage (V_{OUT}) was regulated to 5 V. At this voltage, a 5-Ω and 375 m-Ω power resistors were used to load the UC1825BEVM-CVAL to 1 and 10 A, respectively. For the SEL and SEB, the UC1825B-SP (V_{CC}) was powered up to the maximum absolute operating voltage of 30 V and the load was set to 10 A. During the SET data collection, the device (V_{CC}) was powered up to the minimum recommended operating voltage of 10 V and loaded with 1- and 10-A loads.

The SET events were monitored using a National Instruments™ (NI) PXie-5105 (60 MS/s and 60 MHz of bandwidth) digitizer module and one Tektronix DPO7104C Digital Phosphor Oscilloscope (DPO) with four channels of 40 GS/s and 2.5 GHz of bandwidth. The DPO was used to monitor both the PWM (Outputs), and was triggered from the A-OUT using a pulse width window at ±6% from the nominal value. The NI-PXIe Scope card was used to monitor and trigger from V_{OUT} at using a window trigger set to ±3.5% from the nominal value.

Figure 7 shows a block diagram of the setup used for SEE testing on the UC1825B-SP. Table 3 shows the connections, limits, and compliance values that were used during the characterization. In general, the UC1825B-SP was tested at room temperature (no external heating applied). A die temperature of 125°C was used for SEL testing and was achieved by attaching heaters close to the UC1825B-SP die. The die temperature was monitored during the testing using a thermistor attached close to the die. The device temperature was regulated by using a LakeShore 332 temperature controller in a close-loop. Correlation was achieved using a thermal camera before the SEE characterization.

All boards used for SEE testing were fully checked for functionality and dry runs performed to ensure that the test system was stable under all bias and load conditions prior to being taken to the TAMU facility. All equipment other than the DPO was controlled and monitored using a custom-developed LabVIEW™ program (PXI-RadTest) running on a NI PXIe-8135 controller. During the heavy-ion testing, the LabView control program powered up the UC1825B-SP and UC1825BEVM-CVAL, and set the monitoring functions of the external equipment. After functionality and stability had been confirmed, the beam shutter was opened to expose the device to the heavy-ion beam. The shutter remained open until the target fluence was achieved (determined by external detectors and counters).

During irradiation, the PXIe-5101 scope cards continuously monitored V_{OUT}. When the output voltage exceeds the pre-defined ±3.5% window trigger, data capture was initiated on the scope cards. The sample rate was set to 5 MS/s, in case a trigger occurs – 20-k samples were set to be recorded with a pre-defined 20% reference (percent of the data vector before the trigger happens), however not a single upset exceeding ±3.5 % was observed.

In parallel, the DPO monitored both the PWM (outputs) triggering from a pre-defined ±6% window trigger around the nominal pulse width. The sample rate was set to 20 MS/s with a total capture time of 200 µs total (20 µs/div) and recording 20% or 40 µs before the event. The DPO was set to fast frame during and the counter cleared before each run started. Under this configuration, the scope has a 3.2-µs update rate, indicating that it can re-arm and be ready for the next trigger within 3.2 µs. In addition to monitoring the output voltage and the PWM, the V_{IN} and V_{CC} current as well as the +5-V signal from TAMU were monitored at all times. **No sudden increases in current were observed (outside of normal fluctuations) on any of the test runs indicating that no SEL events occurred during any of the tests.**

Table 3. Equipment Set and Parameters Used for the SEE Testing the UC1825B-SP

PARAMETER	EQUIPMENT USED	CAPABILITY	COMPLIANCE	RANGE OF VALUES USED
V_{IN}	Agilent N6700 PS Channel # 4	5 A	5 A	48 V
V_{CC}	Agilent N6700 PS Channel # 3	3 A	1 A	10 and 30 V
Oscilloscope Card	NI PXie-5105	60 MS/s	-	5 MS/s
Digital Phosphor Oscilloscope	Tektronix DPO7104C	40 GS/s	-	20 MS/s
Digital I/O	NI PXie-6556	200 MHz	-	50 MHz

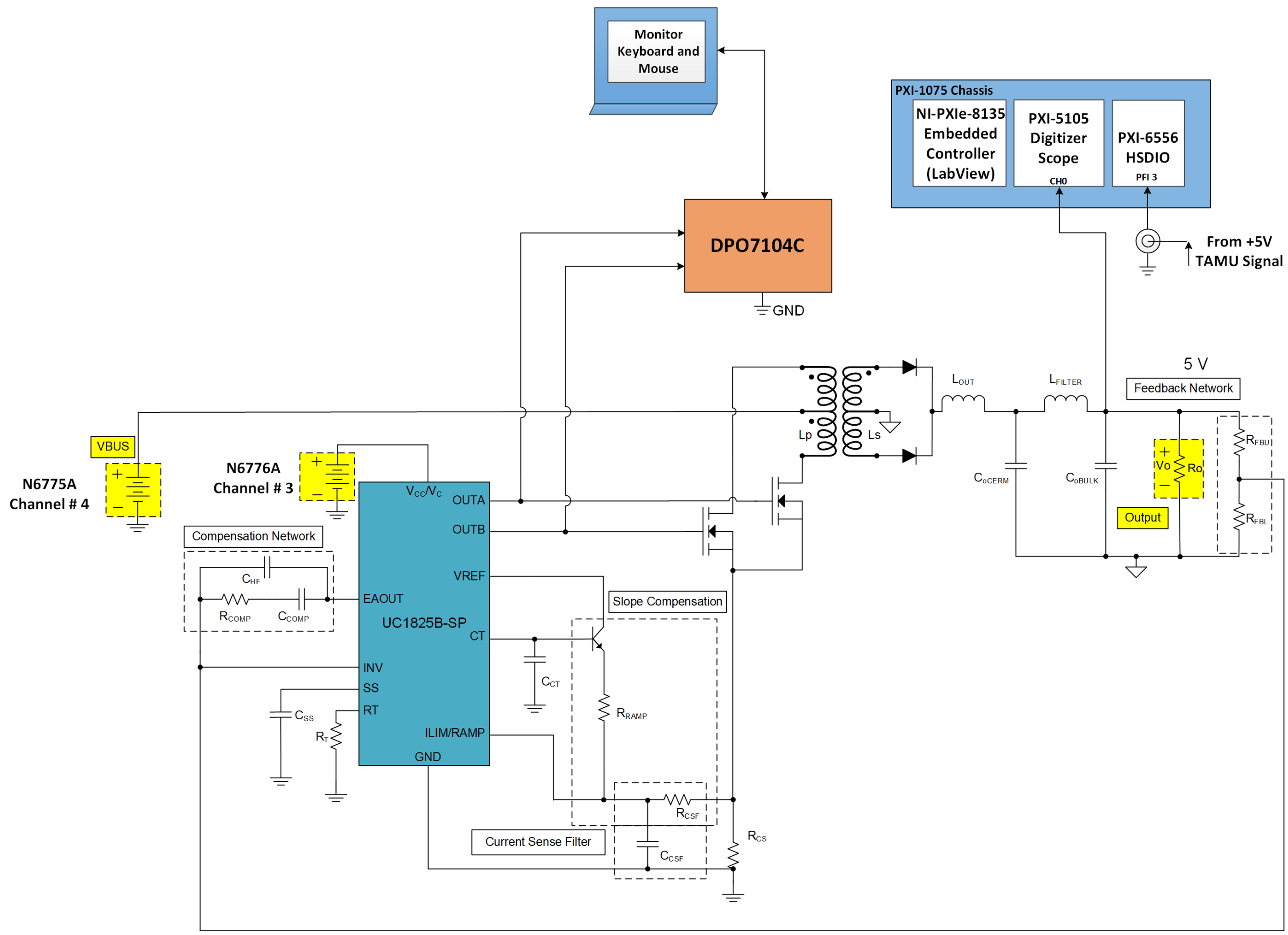

Figure 7. Block Diagram of the Test Setup Used for UC1825B-SP SEE Characterization

7 Destructive Single Event Effects (DSEE)

7.1 Single-Event-Latchup (SEL)

SEL was performed at 125ºC with ^{124}Xe at an angle of incidence of 35º for an LET_{EFF} of 74.1 MeV·cm^2/mg. The heavy-ions were provided by Berkeley 88-inch cyclotron facility (BASE). The device was heated by attaching resistive heaters close to the UC1825B-SP die. Heaters were attached to the UC1825BEVM-CVAL using high-temperature glue. The die temperature was monitored during the testing using a thermistor attached close to the die. The device temperature was regulated by using a LakeShore 332 temperature controller in a close-loop operation.

Prior to the SEE testing session, thermistor and die temperature were correlated by using a thermal infrared (IR) camera. The device was exposed to a Xenon (^{124}Xe) heavy-ion beam incident on the die surface at 35° for an LET_{EFF} of 74.1 MeV·cm^2/mg. A flux of approximately 5.45 × 10^4 ions/cm^2·s and fluence of 10^7 ions/cm^2 was used. The run duration was 217 seconds. V_{CC} was set to the maximum absolute voltage of 30 V while the output voltage of the UC1825BEVM-CVAL was set to 5 V at a 10-A load on the power stage.

Table 4 summarizes the SEL test conditions and results. Figure 8 shows a typical current plot. **No SEL events were observed under the test run, indicating that the UC1825B-SP is SEL-immune at T = 125°C and LET_{EFF} = 74 MeV·cm^2/mg.**

The SEL cross section was calculated based on zero events observed using a 95% confidence interval (see Appendix B for discussion of the cross section calculation method).

$\sigma_{SEL} \leq 3.69 \times 10^{-7}$ cm^2/device at LET_{EFF} = 74 MeV·cm^2/mg, T = 125 °C, and 95% confidence.

Table 4. Summary of UC1825B-SP SEL Test Conditions and Results with T = 125°C

RUN #	UNIT #	TEMPERATURE (°C)	ANGLE OF INCIDENCE (°)	LET_{EFF} (MeV·cm^2/mg)	FLUX (ions/cm^2·s)	FLUENCE (ions/cm^2)	LOAD ON POWER STAGE (A)	SEL EVENTS
1	1	125	35	74.1	5.4 × 10^4	1 × 10^7	10	0

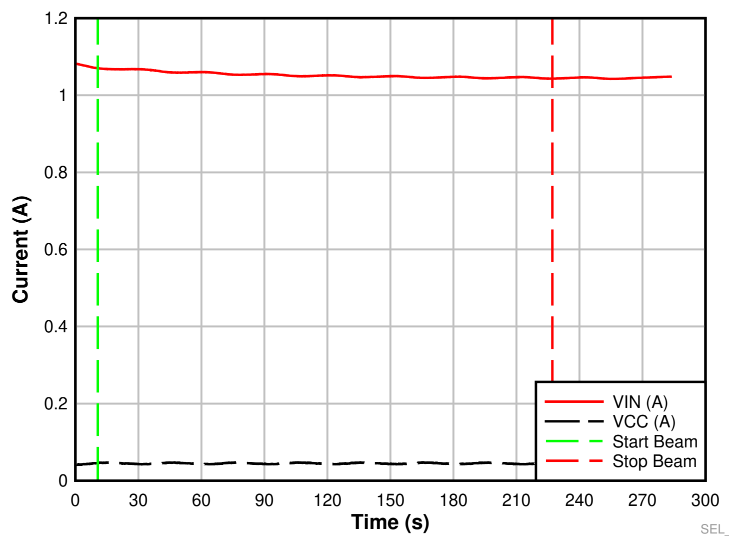

Figure 8. V_{CC} and V_{IN} Current vs Time for SEL Run #1 at T = 125ºC and 74.1 MeV·cm^2/mg

7.2 Single-Event-Burnout (SEB)

SEB was performed at room temperature with ^{124}Xe at an angle of incidence of 35º for an LET_{EFF} of 74.1 MeV·cm^2/mg. The heavy-ions were provided by Berkeley 88-Inch cyclotron facility (BASE). V_{CC} was set to the maximum absolute voltage of 30 V while the output voltage was set to 5 V at a 10-A load on the power stage. Flux of approximately 5.45 × 10^4 ions/cm^2·s and fluence of 10^7 ions/cm^{2}were used per run. The device was evaluated when the DUT was enabled and regulating to 5 V.

Table 5 summarizes the SEB test conditions and results. Figure 9 shows a typical current plot. **No SEB or current spikes events were observed under the test runs, indicating that the UC1825B-SP is SEB-immune at T = 25°C and LET_{EFF} = 74.1 MeV·cm^2/mg.**

The SEB cross section was calculated based on zero events observed, combining accumulated fluence and using a 95% confidence interval (see Appendix B for discussion of the cross section calculation method).

$\sigma_{SEB} \leq 1.84 \times 10^{-7}$ cm^2/device at LET_{EFF} = 74 MeV·cm^2/mg, T = 25°C, and 95% confidence.

Table 5. Summary of UC1825B-SP SEB Test Conditions and Results with T = 25°C and LET_{EFF} = 74 MeV·cm^2/mg

RUN #	UNIT #	TEMPERATURE (°C)	ANGLE OF INCIDENCE (°)	LET_{EFF} (MeV·cm^2/mg)	FLUX (ions/cm^2·s)	FLUENCE (ions/cm^2)	LOAD ON POWER STAGE (A)	SEB EVENTS
2	1	25	35	74.1	5.4 × 10^4	1 × 10^7	10	0
3	1	25	35	74.1	5.4 × 10^4	1 × 10^7	10	0

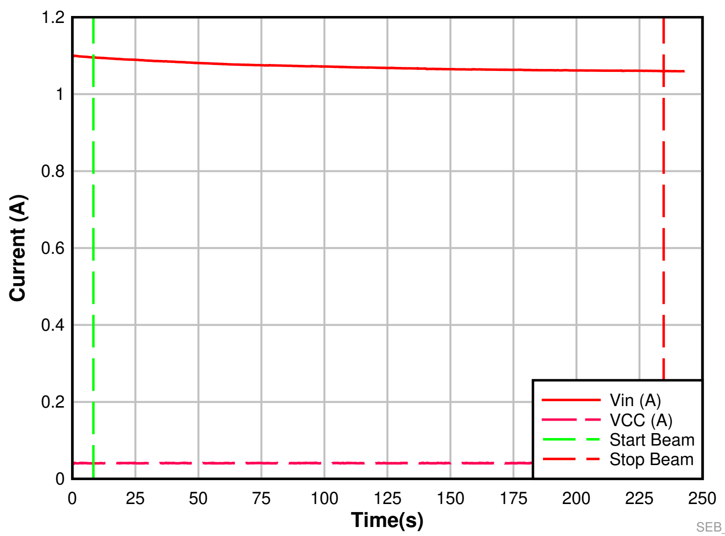

Figure 9. V_{CC} and V_{IN} Current vs Time for SEB Run #2 at T = 125ºC and 74.1 MeV·cm^2/mg

8 Single Event Transients (SET)

SETs were defined as heavy-ion-induced transient variation on the V_{OUT} and on the A-OUT-PWM (output) of the UC1825B-SP device. Variations greater or equal than ± 3.5% on the output voltage and ± 6% on A-OUT were recorded and are referred to here as V_{OUT}-SET and PWM-SET, respectively.

Characterization was conducted at an output voltage of 5 V (nominal) and a load of 1 A and 10 A on the power stage. Transients characterization was conducted at room temperature with ^{63}Cu ions at 0º and 50º angle of incidence for an LET_{EFF} of 20 and 31.3 MeV·cm^2/mg, respectively. Also,^{109}Ag ions at angles of 0º , 30ºand 50º of incidence for an LET_{EFF} of 47.08, 54.48 and 73.77 MeV·cm^2/mg, respectively, were used. See Table 2 for more details on the ions used).

Table 6 summarizes the test conditions and results for the UC1825B-SP SET characterization. Flux of ≈ 10^4 ions/cm^2·s and fluences of ≥ 10^6 ions/cm^2 per run were used. To capture the transients, a window trigger of ±3.5 % around the nominal voltage was used for the V_{OUT}-SET. For the PWM-SET a Pulse-Width trigger of ±6 % around the nominal positive pulse-width value was used. **At the trigger conditions used for V_{OUT}-SET, not a single SET was observed**.

On the PWM-SET upsets were observed and recorded for post-processing. The trigger condition was set to capture data any time the pulse width exceeds the ±6% window on the A-OUT signal on the DPO. With any upset observed, the A-OUT and B-OUT signals were recorded.

Data was post-processed to ±25%, however, for most of the runs, only 500 upsets (or waveforms) of the total number of upsets was saved into the memory. **However even when not all waveforms were saved, the correct count (or triggers) was recorded.**

To determine the total number of waveforms that exceed ±25%, on the runs that the complete data set was not available a linear interpolation was used. For those runs, the number of upsets was found by rounding to the nearest integer of the result from:

$$N \geq |25\%| = \left(\frac{N \geq |25\%|}{N \geq |6\%|}\right) \times \left(N \geq |6\%|\right) \tag{1}$$

where:

N ≥ |25%| - is the total number of waveforms from the available data , in which the positive pulse width exceeds the ±25% deviation from the nominal value.

N ≥ |6%| - is the counter value for the total number of waveforms that exceed the positive pulse width exceeds ±6% from the nominal value.

Per the UC1825B-SP design, A and B PWM outputs are inverted in phase. As heavy-ions can dynamically change the proper state of the outputs, the data was verified for upsets in which both outputs were on at the same time. To convert the analog PWM signal into Boolean, the data was normalized comparing the time domain voltage value against the mid-level value of the PWM signals (in this case, mid-level= 5V). The following formula was applied to the time domain voltage waveforms:

$$\text{Signal State} = \begin{cases} 1 & \text{if } V \geq \text{Mid} - \text{Level} \\ 0 & \text{otherwise} \end{cases} \tag{2}$$

After the transformation, a bit-wise AND gate was performed on the data of the A-OUT and BOUT waveforms. When logical *ones* were observed on the resultant vector, an upset in which both outputs were on was counted, also the consecutive logical *ones* were used to determine the duration of these upsets. Just one upset showing a duration of 2 samples (sampled at 50 ns), all others showed a duration of 1 sample. **It is important to mention that even when this kind of upsets were observed, destructive or permanent damage was not observed on the switching FETS of the tested EVMs.**

On incomplete data sets, data was scale up linearly as mentioned before. The number of observed upsets was also scaled up, per Equation 1.

The A-OUT PWM output cross section and Weibull fit plot for 10- and 1-A loads is shown in Figure 10 and Figure 11, respectively. The Weibull fit parameters for the A-OUT PWM-SET (≥ |6%| and ≥ |25%|) and both *on* for 10- and 1-A loads, per Equation 3 is shown in Table 7.

$$\sigma(LET) = \sigma_{SAT} \times \left(1 - e^{\left(-\frac{LET - Onset}{W}\right)^{s}}\right) \tag{3}$$

Figure 12 shows a histogram of all the saved upsets in A-OUT. The data was normalized per Equation 4. Time domain plots for the observed worst-case positive and negative pulse width deviation from the nominal value are shown on Figure 13 and Figure 14, respectively. A positive deviation is equivalent to an upset in which the pulse width deviation was greater than the nominal pulse width value. Negative deviation upsets were considered as an upset in which pulse width deviation was lower than the nominal pulse width value. As can be observed, the worst-case negative deviation upset is also an upset in which both A-OUT and BOUT, were on at the same time. The observed worst-case time duration upset in which both outputs were on, is shown in Figure 15, the upset duration is 100 ns.

$$\text{Normalized PWM} = \left(\frac{\text{Pulse Width} \geq |25\%| - \text{Nominal PulseWidth}}{\text{Nominal PulseWidth}} \right) \times 100\% \quad (4)$$

The SET upper bound cross section for the V_{OUT} and PWM (Outputs) was calculated using a 95% confidence interval and combining the fluence (see Appendix B for discussion of the cross section calculation method).

$\sigma_{SET\text{-}VOUT@3.5\%} \leq 6.15 \times 10^{-7}$ cm²/device at LET_{EFF} = 74 MeV·cm²/mg, T = 25 °C , Load = 1 and 10 A and 95% confidence.

$\sigma_{SET\text{-}PWM@6\%} \leq 4.59 \times 10^{-3}$ cm²/device at LET_{EFF} = 74 MeV·cm²/mg, T = 25 °C, Load = 1 and 10 A and 95% confidence.

$\sigma_{SET\text{-}PWM@25\%} \leq 1.42 \times 10^{-3}$ cm²/device at LET_{EFF} = 74 MeV·cm²/mg, T = 25 °C, Load = 1 and 10 A and 95% confidence.

$\sigma_{SET\text{-}PWM@Both\ On} \leq 2.5 \times 10^{-5}$ cm²/device at LET_{EFF} = 74 MeV·cm²/mg, T = 25 °C, Load = 1 and 10 A and 95% confidence.

Table 6. Summary of UC1825B-SP SET Test Conditions and Results With T = 25°C

RUN #	UNIT #	ION	ANGLE OF INCIDENCE (°)	LET_{EFF} (MeV·cm²/mg)	FLUX (ions/cm²·s)	FLUENCE (ions/cm²)	Load (A)	PWM UPSETS > |6%|(#)	PWM UPSETS > |25%|(#)	Both On (#)
4	2	Cu	0	19.99	1.1×10^4	3×10^6	10	3610	1177	0
5	2	Cu	50	31.3	1.11×10^4	3×10^6	10	5241	2244	0
6	1	Ag	0	47.1	1.33×10^4	3×10^6	10	7142	2686	0
7	1	Ag	0	47.1	1.27×10^4	1.02×10^6	10	2426	1000	10
8	1	Ag	30	54.48	1.33×10^4	3×10^6	10	7359	3059	15
9	1	Ag	50	73.8	1.29×10^4	1×10^6	10	3059	1394	19
10	1	Ag	50	73.8	1.29×10^4	2×10^6	10	6033	2752	39
11	2	Cu	0	19.99	1.08×10^4	3×10^6	1	7370	855	0
12	2	Cu	50	31.3	1.10×10^4	3×10^6	1	10781	1876	0
13	1	Ag	0	47.1	1.26×10^4	3.01×10^6	1	10542	3058	0
14	1	Ag	30	54.48	1.24×10^4	3.01×10^6	1	11313	3394	0
15	1	Ag	50	73.8	1.23×10^4	3.01×10^6	1	13530	3518	55

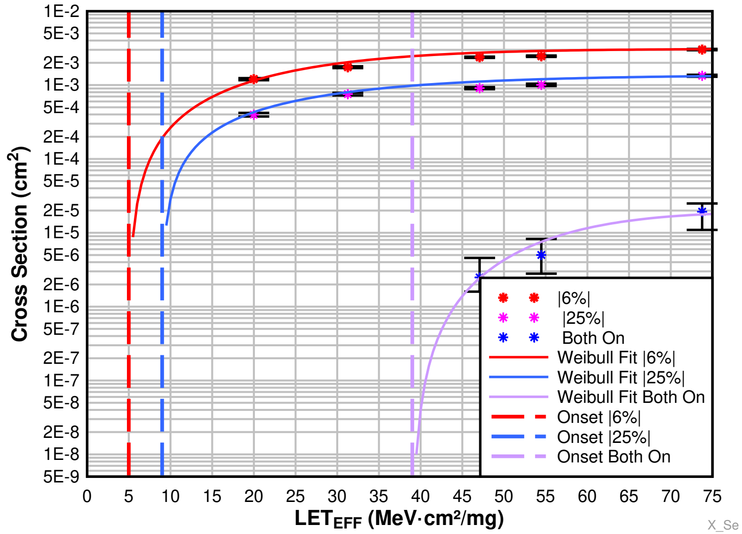

Figure 10. A-OUT Cross Section vs LET for the 10-A Load on the UC1825B-SP

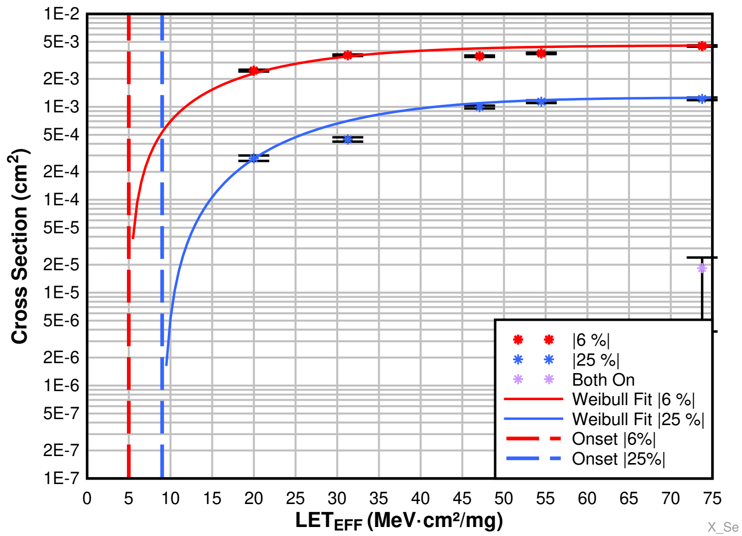

Figure 11. A-OUT Cross Section vs LET for the 1-A Load on the UC1825B-SP

Table 7. Weibull Fit Parameters for the PWM Cross Section for Upsets ≥ 6%, 25%, and Both On

σ_{SAT}	ONSET	W	s	LOAD	CONDITION
3.09×10^{-3}	5	25	1.5	10	> |6%|
1.42×10^{-3}	9	25	1.2	10	> |25%|
1.93×10^{-5}	39	22	2	10	Both On
4.59×10^{-3}	5	20	1.3	1	> |6%|
1.21×10^{-3}	9	25	1.7	1	> |25%|

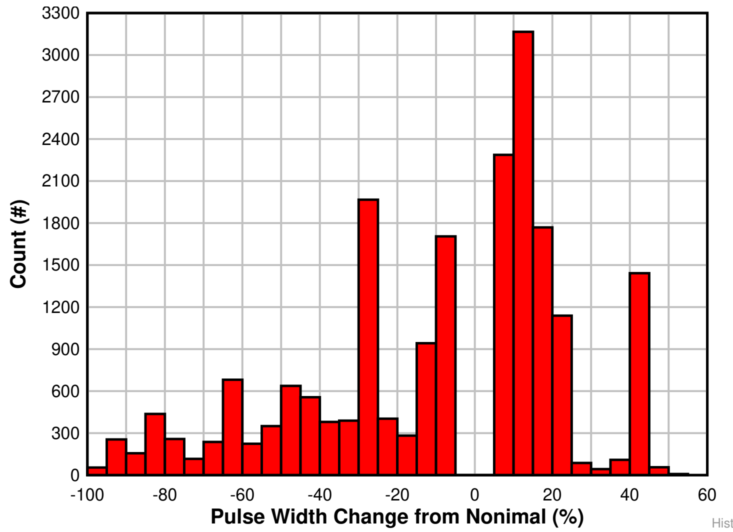

Figure 12. Histogram of all Saved Normalized Upsets in the A-OUT PWM Output ≥ |6%|

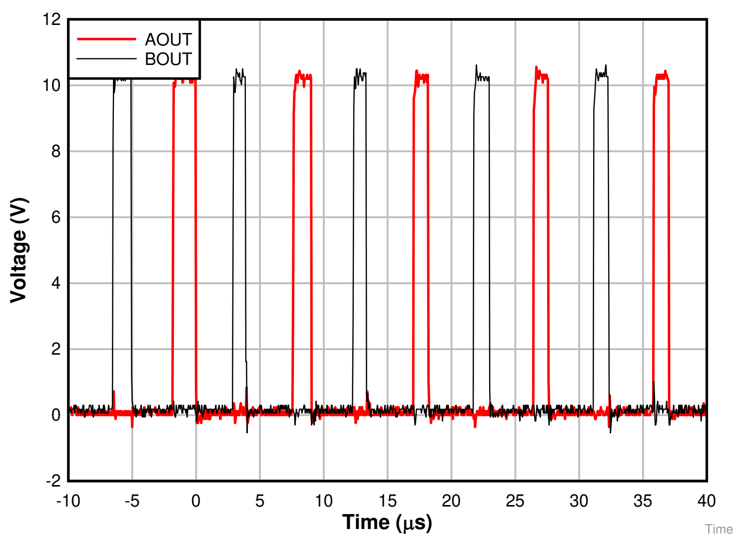

Figure 13. Worst-Case Positive Deviation from the Nominal Pulse Width on A-OUT

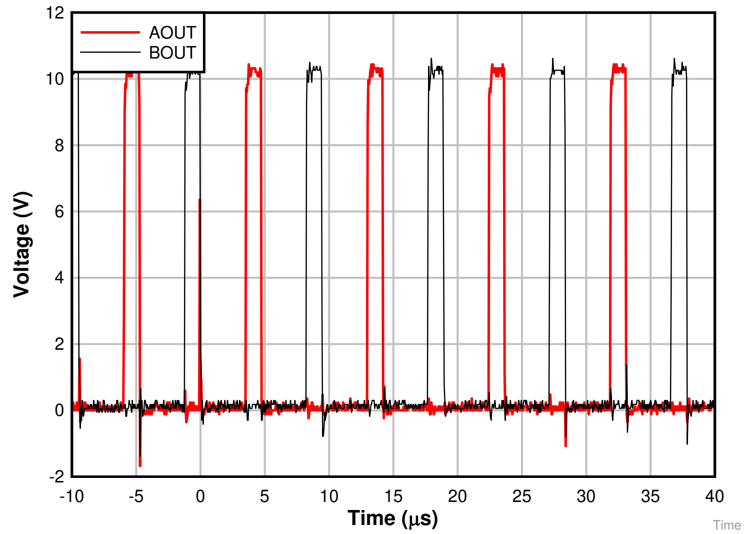

Figure 14. Worst-Case Negative Deviation From the Nominal Pulse Width on A-OUT

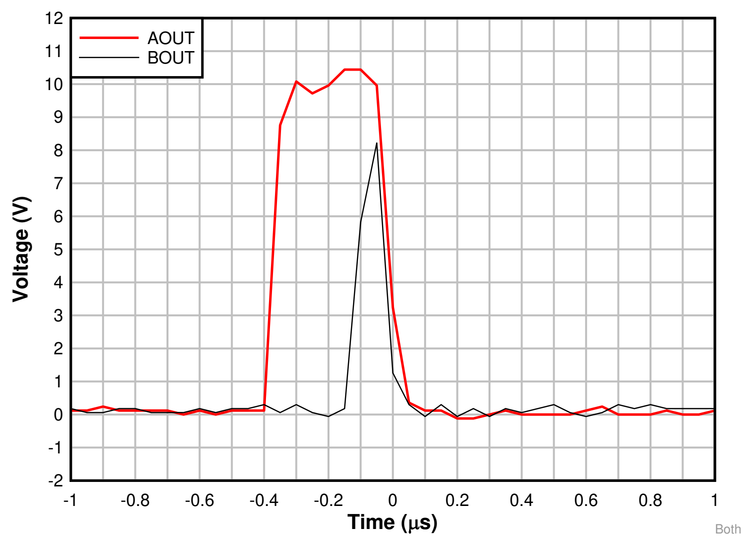

Figure 15. Worst Case Both On Upset (Duration of 100 ns)

9 Event Rate Calculations

Events rates were calculated for LEO (ISS) and GEO environments by combining CREME96 orbital integral flux estimations. A minimum shielding of 100 mils (2.54 mm) of aluminum and "worst week" solar activity was assumed. "Worst Week" is similar to 99% upper bound for the environment. With zero upsets for SEL and SEB and SET-V_{OUT} ≥ 3.5 , the error rate was calculated using the upper bound cross section and the integral flux at 74 (for SEL and SEB/SEGR) and 73 (for SET-V_{OUT} ≥ 3.5 %) MeV·cm^2/mg. Otherwise, the respective on-set and the upper bound was used.

Table 8. SEL Event Rate Calculations for Worst-Case LEO and GEO Orbits

ORBIT TYPE	ONSET (MeV·cm^2/mg)	CREME96 INTEGRAL FLUX (/day·cm^2)	SATURATION CROSS SECTION (cm^2)	EVENT RATE (/DAY)	EVENT RATE (FIT)	MTBE (YEARS)
LEO (ISS)	74.4	6.64×10^{-5}	3.69×10^{-7}	2.45×10^{-11}	1.02×10^{-3}	1.12×10^{8}
GEO		1.88×10^{-4}		6.92×10^{-11}	2.88×10^{-3}	3.96×10^{7}

Table 9. SEB Event Rate Calculations for Worst-Case LEO and GEO Orbits

ORBIT TYPE	ONSET (MeV·cm^2/mg)	CREME96 INTEGRAL FLUX (/day·cm^2)	SATURATION CROSS SECTION (cm^2)	EVENT RATE (/DAY)	EVENT RATE (FIT)	MTBE (YEARS)
LEO (ISS)	74.4	6.64×10^{-5}	1.84×10^{-7}	1.22×10^{-11}	5.10×10^{-4}	2.24×10^{8}
GEO		1.88×10^{-4}		3.46×10^{-11}	1.44×10^{-3}	7.92×10^{7}

Table 10. V_{OUT} ≥ |3.5%| SET Event Rate Calculations for Worst-Case LEO and GEO Orbits

ORBIT TYPE	ONSET (MeV·cm^2/mg)	CREME96 INTEGRAL FLUX (/day·cm^2)	SATURATION CROSS SECTION (cm^2)	EVENT RATE (/DAY)	EVENT RATE (FIT)	MTBE (YEARS)
LEO (ISS)	73	7.15×10^{-5}	6.15×10^{-7}	4.39×10^{-11}	1.83×10^{-3}	6.23×10^{7}
GEO		2×10^{-4}		1.24×10^{-10}	5.18×10^{-3}	2.2×10^{7}

Table 11. PWM ≥ |6%| @ 10-A Load SET Event Rate Calculations for Worst-Case LEO and GEO Orbits

ORBIT TYPE	ONSET (MeV·cm^2/mg)	CREME96 INTEGRAL FLUX (/day·cm^2)	SATURATION CROSS SECTION (cm^2)	EVENT RATE (/DAY)	EVENT RATE (FIT)	MTBE (YEARS)
LEO (ISS)	5	138.14	3.09×10^{-3}	0.427	1.78×10^{7}	6.41×10^{-3}
GEO		1.24×10^{3}		38.4	1.6×10^{8}	0.713×10^{-3}

Table 12. PWM ≥ |25%| @ 10-A Load SET Event Rate Calculations for Worst-Case LEO and GEO Orbits

ORBIT TYPE	ONSET (MeV·cm^2/mg)	CREME96 INTEGRAL FLUX (/day·cm^2)	SATURATION CROSS SECTION (cm^2)	EVENT RATE (/DAY)	EVENT RATE (FIT)	MTBE (YEARS)
LEO (ISS)	9	42.47	1.42×10^{-3}	0.061	2.52×10^{6}	0.045
GEO		355.62		0.51	2.11×10^{7}	0.005

Table 13. PWM Both on @ 10-A Load SET Event Rate Calculations for Worst-Case LEO and GEO Orbits

ORBIT TYPE	ONSET (MeV·cm^2/mg)	CREME96 INTEGRAL FLUX (/day·cm^2)	SATURATION CROSS SECTION (cm^2)	EVENT RATE (/DAY)	EVENT RATE (FIT)	MTBE (YEARS)
LEO (ISS)	39	9.15×10^{-4}	1.93×10^{-5}	1.84×10^{-8}	0.0765	1.49×10^{5}
GEO		0.0035		6.76×10^{-8}	2.82	4.05×10^{4}

Table 14. PWM ≥ |6%| @ 1-A Load SET Event Rate Calculations for Worst-Case LEO and GEO Orbits

ORBIT TYPE	ONSET ($MeV·cm^2/mg$)	CREME96 INTEGRAL FLUX ($/day·cm^2$)	SATURATION CROSS SECTION (cm^2)	EVENT RATE (/DAY)	EVENT RATE (FIT)	MTBE (YEARS)
LEO (ISS)	5	138.14	4.59×10^{-3}	0.634	2.64×10^{7}	4.32×10^{-3}
GEO		1.24×10^{3}		5.7	2.38×10^{8}	4.8×10^{-4}

Table 15. PWM ≥ |25%| @ 1-A Load SET Event Rate Calculations for Worst-Case LEO and GEO Orbits

ORBIT TYPE	ONSET ($MeV·cm^2/mg$)	CREME96 INTEGRAL FLUX ($/day·cm^2$)	SATURATION CROSS SECTION (cm^2)	EVENT RATE (/DAY)	EVENT RATE (FIT)	MTBE (YEARS)
LEO (ISS)	9	42.47	1.21×10^{-3}	5.15×10^{-2}	2.15×10^{6}	0.053
GEO		355.62		4.31×10^{-1}	1.8×10^{7}	0.006

Table 16. PWM Both on @ 1-ALoad SET Event Rate Calculations for Worst-Case LEO and GEO Orbits

ORBIT TYPE	ONSET ($MeV·cm^2/mg$)	CREME96 INTEGRAL FLUX ($/day·cm^2$)	SATURATION CROSS SECTION (cm^2)	EVENT RATE (/DAY)	EVENT RATE (FIT)	MTBE (YEARS)
LEO (ISS)	73	7.15×10^{-5}	2.39×10^{-5}	1.71×10^{-9}	7.11×10^{-2}	1.61×10^{6}
GEO		2.02×10^{-4}		4.83×10^{-9}	2.01×10^{-1}	5.67×10^{5}

10 Summary

The purpose of this report is to summarize the UC1825B-SP SEE performance under heavy-ion irradiation. The data shows the device is SEL (T = 125°C) and SEB (T = 25°C)-free up to 74 $MeV·cm^2/mg$ and across the full electrical specifications. Also zero upsets were observed for SET-V_{OUT} ≥ 3.5 % from the nominal voltage under the configuration tested. The SET cross section for the PWM output upsets ≥ |6% and 25%| above the nominal pulse width and both-on is also presented and discussed. For the purpose of reference, the orbit rate calculation for the LEO (ISS) and GEO for the SEL, SEB and SET was discussed.

Total Ionizing Dose From SEE Experiments

The production UC1825B-SP POL is rated to a total ionizing dose (TID) of 100 krad(Si). In the course of the SEE testing, the heavy-ion exposures delivered ≈ 10 krad(Si) per 10^7 ions/cm^2 run. The cumulative TID exposure for each device respectively, over all runs they underwent, was determined to be below the 100 krad(Si). All qualified production devices used in the studies described in this report were fully-functional after the heavy-ion SEE testing was completed.

Confidence Interval Calculations

For conventional products where hundreds of failures are seen during a single exposure, one can determine the average failure rate of parts being tested in a heavy-ion beam as a function of fluence with high degree of certainty and reasonably tight standard deviation, and thus have a good deal of confidence that the calculated cross section is accurate.

With radiation-hardened parts however, determining the cross section becomes more difficult since often few, or even, no failures are observed during an entire exposure. Determining the cross section using an average failure rate with standard deviation is no longer a viable option, and the common practice of assuming a single error occurred at the conclusion of a null-result can end up in a greatly underestimated cross section.

In cases where observed failures are rare or non-existent, the use of confidence intervals and the chi-squared distribution is indicated. The Chi-Squared distribution is particularly well-suited for the determination of a reliability level when the failures occur at a constant rate. In the case of SEE testing, where the ion events are random in time and position within the irradiation area, one expects a failure rate that is independent of time (presuming that parametric shifts induced by the total ionizing dose do not affect the failure rate), and thus the use of chi-squared statistical techniques is valid (since events are rare, an exponential or Poisson distribution is usually used).

In a typical SEE experiment, the device-under-test (DUT) is exposed to a known, fixed fluence (ions/cm^2) while the DUT is monitored for failures. This is analogous to fixed-time reliability testing, and more specifically, time-terminated testing, where the reliability test is terminated after a fixed amount of time whether or not a failure has occurred (in the case of SEE tests fluence is substituted for time and hence it is a fixed fluence test) [14]. Calculating a confidence interval specifically provides a range of values which is likely to contain the parameter of interest (the actual number of failures/fluence). Confidence intervals are constructed at a specific confidence level. For example, a 95% confidence level implies that if a given number of units were sampled numerous times and a confidence interval estimated for each test, the resulting set of confidence intervals would bracket the true population parameter in about 95% of the cases.

To estimate the cross section from a null-result (no fails observed for a given fluence) with a confidence interval, start with the standard reliability determination of lower-bound (minimum) mean-time-to-failure for fixed-time testing (an exponential distribution is assumed):

$$\mathrm{MTTF} = \frac{2nT}{\chi^2_{2(d+1);100\left(1-\frac{\alpha}{2}\right)}}$$

where

- *MTTF* is the minimum (lower-bound) mean-time-to-failure
- *n* is the number of units tested (presuming each unit is tested under identical conditions)
- *T*, is the test time
- x^2 is the chi-square distribution evaluated at 100 (1 – α / 2) confidence level
- d is the degrees-of-freedom (the number of failures observed) (5)

With slight modification for this purpose, invert the inequality and substitute *F* (fluence) in the place of *T*:

$$MFTF = \frac{2nF}{\chi^2_{2(d+1);100\left(1-\frac{\alpha}{2}\right)}}$$

where

- *MFTF* is mean-fluence-to-failure
- *F* is the test fluence
- x^2 is the chi-square distribution evaluated at 100 (1 – α / 2) confidence
- *d* is the degrees-of-freedom (the number of failures observed) (6)

The inverse relation between MTTF and failure rate is mirrored with the MFTF. Thus, the upper-bound cross section is obtained by inverting the MFTF:

$$\sigma = \frac{\chi^2_{2(d+1);100\left(1-\frac{\alpha}{2}\right)}}{2nF} \tag{7}$$

Assume that all tests are terminated at a total fluence of 10^6 ions/cm^2. Also assume that we have a number of devices with very different performances that are tested under identical conditions. Assume a 95% confidence level (σ = 0.05). Note that as *d* increases from 0 events to 100 events, the actual confidence interval becomes smaller, indicating that the range of values of the true value of the population parameter (in this case the cross section) is approaching the mean value + 1 standard deviation. This makes sense when one considers that as more events are observed the statistics are improved such that uncertainty in the actual device performance is reduced.

Table 17. Experimental Example Calculation of Mean-Fluence-to-Failure (MFTF) and σ Using a 95% Confidence Interval (1)

DEGREES-OF-FREEDOM (d)	2(d + 1)	χ^2 AT 95%	CALCULATED CROSS SECTION (cm^2)		
			UPPER-BOUND AT 95% CONFIDENCE	MEAN	AVERAGE + STANDARD DEVIATION
0	2	7.38	3.69E–06	0.00E+00	0.00E+00
1	4	11.14	5.57E–06	1.00E–06	2.00E–06
2	6	14.45	7.22E–06	2.00E–06	3.41E–06
3	8	17.53	8.77E–06	3.00E–06	4.73E–06
4	10	20.48	1.02E–05	4.00E–06	6.00E–06
5	12	23.34	1.17E–05	5.00E–06	7.24E–06
10	22	36.78	1.84E–05	1.00E–05	1.32E–05
50	102	131.84	6.59E–05	5.00E–05	5.71E–05
100	202	243.25	1.22E–04	1.00E–04	1.10E–04

(1) Using a 95% confidence for several different observed results (d = 0, 1, 2...100 observed events during fixed-fluence tests) assuming 10^6 ion/cm^2 for each test.

Orbital Environment Estimations

To calculate on-orbit SEE event rates, one needs both the device SEE cross section and the flux of particles encountered in a particular orbit. Device SEE cross sections are usually determined experimentally while flux of particles in orbit is calculated using various codes. For the purpose of generating some event rates, a Low-Earth Orbit (LEO) and a Geostationary-Earth Orbit (GEO) were calculated using Cosmic Ray Effects on Micro-Electronics (CREME96). CREME96 code is a suite of programs [15][16] that enable estimation of the radiation environment in near-Earth orbits. CREME96 is one of several tools available in the aerospace industry to provide accurate space environment calculations. Over the years since its introduction, the CREME models have been compared with on-orbit data and demonstrated their accuracy. In particular, CREME96 incorporates realistic “worst-case” solar particle event models, where fluxes can increase by several orders-of-magnitude over short periods of time.

For the purposes of generating conservative event rates, the worst-week model (based on the biggest solar event lasting a week in the last 45 years) was selected, which has been equated to a 99%-confidence level worst-case event [17][18]. The integrated flux includes protons to heavy ions from solar and galactic sources. A minimal shielding configuration is assumed at 100 mils (2.54 mm) of aluminum. Two orbital environments were estimated, that of the International Space Station (ISS), which is LEO, and the GEO environment. Figure 16 shows the integrated flux (from high LET to low) for these two environments.

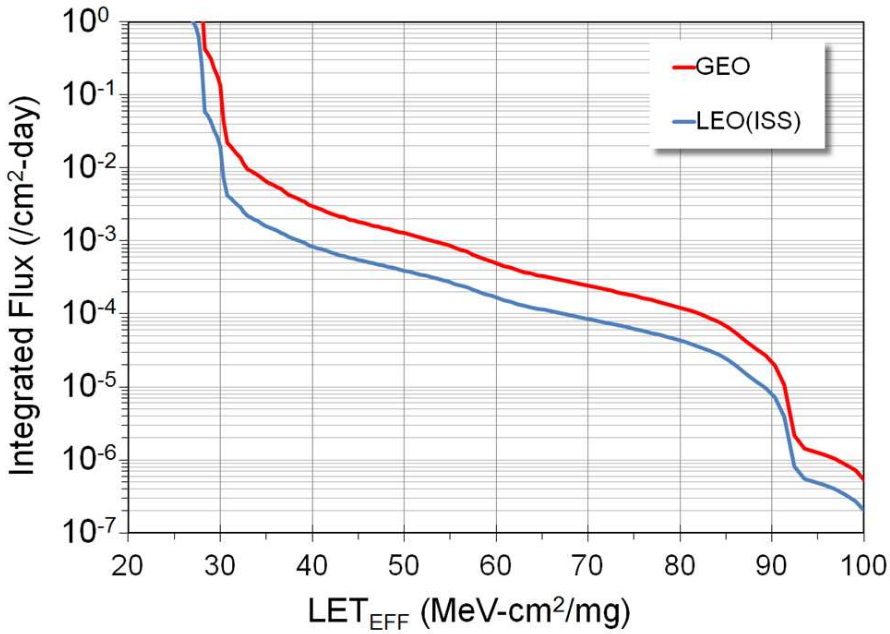

(1) LEO(ISS) (blue) and a GEO (red) environment as calculated by CREME96, assuming worst-week and 100 mils (2.54 mm) of aluminum shielding.

Figure 16. Integral Particle Flux vs LET_{EFF}

Using this data, you can extract integral particle fluxes for any arbitrary LET of interest. To simplify the calculation of event rates, assume that all cross section curves are square – meaning that below the onset LET, the cross section is identically zero while above the onset LET the cross section is uniformly equal to the saturation cross section. Figure 17 illustrates the approximation, with the green curve being the actual Weibull fit to the data with the “square” approximation shown as the red-dashed line. This allows you to calculate event rates with a single multiplication, the event rate becoming simply the product of the integral flux at the onset LET, and the saturation cross section. Obviously this leads to an overestimation of the event rate since the area under the square approximation is larger than the actual cross section curve – but for the purposes of calculating upper-bound event rate estimates, this modification avoids the need to do the integral over the flux and cross-section curves.

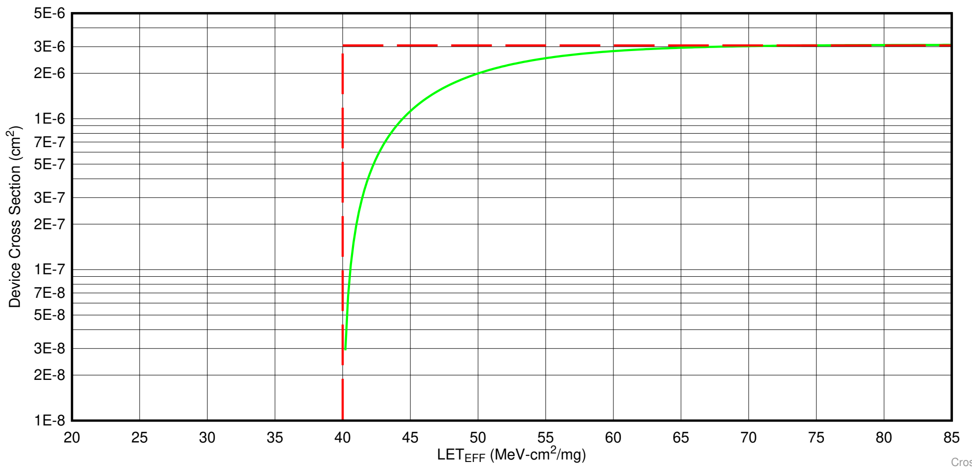

(1) Weibull Fit (green) is “simplified” with the use of a square approximation (red dashed line).

Figure 17. Device Cross Section vs LET_{EFF}

To demonstrate how the event rates in this report were calculated, assume that you wish to calculate an event rate for a GEO orbit for the device whose cross section is shown in Figure 17. Using the red curve in Figure 16 and the onset LET value obtained from Figure 17 (approximately 40 MeV-cm^2/mg), you find the GEO integral flux to be approximately 2.97 × 10^{-3} ions/cm^2-day. The event rate is the product of the integral flux and the saturation cross section in Figure 17 (approximately 3.09 × 10^{-6} cm^2):

$$GEO\ Event\ Rate = \left(2.97 \times 10^{-3} \frac{ions}{cm^2 \times day}\right) \times (3.09 \times 10^{-6}\ cm^2) = 9.17 \times 10^{-9}\ \frac{events}{day} \quad (8)$$

$$GEO\ Event\ Rate = 3.82 \times 10^{-10} \frac{events}{hr} = 0.382\ FIT \quad (9)$$

$$MTBF = 298901\ Years\ ! \quad (10)$$

References

(1) J.L. Titus, G.H. Johnson, R.D. Schrimpf, K.F. Galloway, "Single event burnout of power bipolar junction transistors," IEEE Trans. on Nuclear Science, vol. NS-38, no. 6, pp. 1315-1322, 1991.

(2) S. Kuboyama, T. Suzuki, T. Hirao and S. Matsuda, "Mechanism for single-event burnout of bipolar transistors," in IEEE Transactions on Nuclear Science, vol. 47, no. 6, pp. 2634-2639, Dec 2000.

(3) TAMU Radiation Effects Facility website. https://cyclotron.tamu.edu/ref/.

(4) 88-Inch Berkeley Accelerator Space Effects (BASE) website.http://cyclotron.lbl.gov/.

(5) M. K. Covo et al., "88-Inch Cyclotron: The one-stop facility for electronics radiation testing," 2017 IEEE International Workshop on Metrology for AeroSpace (MetroAeroSpace), Padua, 2017, pp. 484-488.

(6) G. H. Johnson, R. D. Schrimpf, K. F. Galloway, and R. Koga, “Temperature dependence of single-event burnout in n-channel power MOSFETs [for space application],” *IEEE Trans. Nucl. Sci.*, Vol. 39(6), Dec. 1992, pp. 1605–1612.

(7) D. K. Nichols, J. R. Coss, and K. P. McCarty, “Single event gate rupture in commercial power MOSFETs,” Radiation and its Effects on Components and Systems, Sept. 1993, pp. 462–467.

(8) M. Shoga and D. Binder, “Theory of Single Event Latchup in Complementary Metal-Oxide Semiconductor ICs”, *IEEE Trans. Nucl. Sci.*, Vol. 33(6), Dec. 1986, pp. 1714–1717.

(9) G. Bruguier and J.M. Palau, “Single particle-induced latchup”, *IEEE Trans. Nucl. Sci.*, Vol. 43(2), Mar. 1996, pp. 522–532.

(10) J. M. Hutson, R. D. Schrimpf, and L. W. Massengill, “The effects of scaling and well and substrate contact placement on single event latchup in bulk CMOS technology,” in Proc. RADECS, Sept. 2005, pp. PC24-1–PC24-5.

(11) N. A. Dodds, J. M. Hutson, J. A. Pellish, et al., “Selection of Well Contact Densities for Latchup-Immune Minimal-Area ICs, *IEEE Trans. Nucl. Sci.*, Vol. 57(6), Dec. 2010, pp. 3575–3581.

(12) D. B. Estreich and A. Ochoa, Jr., and R. W. Dutton, “An Analysis of Latch-Up Prevention in CMOS IC's Using an Epitaxial-Buried Layer Process*, Proceed. IEEE Elec. Dev. Meeting, 24, Dec. 1978, pp. 230–234.

(13) R. Krithivasan, et al., “Application of RHBD techniques to SEU hardening of Third-Generation SiGe HBT Logic Circuits,” *IEEE Trans. Nucl. Sci.*, Vol. 53(6), Dec. 2006, pp. 3400–3407.

(14) P. C. Adell, R. D. Schrimpf, B. K. Choi, W. T. Holman, J. P. Attwood, C. R. Cirba, and K. F. Galloway, “Total-Dose and Single-Event Effects in Switching DC/DC Power Converters,” *IEEE Trans. Nucl. Sci.* Vol. 49(6), Dec. 2002, pp. 3217–3221.

(15) R. L. Pease, “Modeling Single Event Transients in Bipolar Linear Circuits,” *IEEE Trans. Nucl. Sci.*, Vol. 55(4), Aug. 2008, pp. 1879–1890.

(16) R. Lveugle and A. Ammari, “Early SEU Fault Injection in Digital, Analog and Mixed Signal Circuits: a Global Flow,” Proc. of Design, Automation and Test in Europe Conf., 2004, pp. 1530–1591.

(17) TAMU Radiation Effects Facility website. http://cyclotron.tamu.edu/ref/

(18) “The Stopping and Range of Ions in Matter” (SRIM) software simulation tools website. http://www.srim.org/index.htm#SRIMMENU

(19) D. Kececioglu, “Reliability and Life Testing Handbook”, Vol. 1, PTR Prentice Hall, New Jersey,1993, pp. 186–193.

(20) https://creme.isde.vanderbilt.edu/CREME-MC

(21) A. J. Tylka, et al., "CREME96: A Revision of the Cosmic Ray Effects on Micro-Electronics Code", *IEEE Trans. Nucl. Sci.*, Vol. 44(6), 1997, pp. 2150–2160.

(22) A. J. Tylka, W. F. Dietrich, and P. R. Boberg, “Probability distributions of high-energy solar-heavy-ion fluxes from IMP-8: 1973–1996”, *IEEE Trans. Nucl. Sci.*, Vol. 44(6), Dec. 1997, pp. 2140–2149.

(23) A. J. Tylka, J. H. Adams, P. R. Boberg, et al.,“CREME96: A Revision of the Cosmic Ray Effects on Micro-Electronics Code”, *IEEE Trans. Nucl. Sci.*, Vol. 44(6), Dec. 1997, pp. 2150–2160.